SPATIAL FOCUSING INSPIRED 5G SPECTRUM SHARING

Chunxiao Jiang*, Beibei Wang*, Yi Han*, Zhung-Han Wu*, K. J. Ray Liu*

*Department of Electrical and Computer Engineering, University of Maryland, College Park, MD 20742, USA

E-mail: chx.jiang@gmail.com, {bebewang, yhan1990, zhwu, kjrliu}@umd.edu

ABSTRACT

Next-generation wireless networks are expected to support exponentially increasing number of users and demands of data, which all rely on the essential media: spectrum. Notice that the 5G networks are featured either by wide bandwidth like mmWave systems, or by large-scale antennas like massive MIMO. We find those two trends, together with waveforming or beamforming, can lead to a common phenomenon: the spatial focusing effect. Based on this focusing effect, we propose a general spatial spectrum sharing framework that enables concurrent multi-users spectrum sharing without the requirement of orthogonal resource allocation. Simulation results show that both TR wideband and massive MIMO system can achieve equivalently high throughput performance with the spatial spectrum sharing scheme.

Index Terms— Spectrum sharing, spatial focusing, massive MIMO, time reversal, network association.

1. INTRODUCTION

Spectrum sharing has been continuously attracting the research community [1]. In the literature, spectrum sharing for 5G networks has been preliminarily studied in [2]-[7]. The "software defined network" (SDN) technology was applied to the heterogeneous networks (HetNets) spectrum sharing in [2]. The prediction of the spectrum usage was introduced in [3] and another prediction of primary users' moving trajectory was proposed in [4]. Joseph Mitola III introduced a concept of public-private spectrum sharing in [5], while Kwan Ng *et al.* proposed to simultaneously utilize licensed and unlicensed bands to improve the energy efficiency in [6]. From the perspectives of operators, the authors in [7] designed a coordination protocol among operators based on reciprocity modeling.

As one can see from the aforementioned works, the researchers have attempted to re-treat the spectrum sharing problem by incorporating new technologies and concepts. Different from those existing works, we focus on a special phenomenon in 5G networks: the spatial focusing effect, especially when the bandwidth becomes wider and wider as in mmWave or the scale of antennas becomes larger and larger as in massive MIMO. This focusing effect is fundamentally due to the decreased correlation between the channel states of two different locations. On one hand, the massive number of antennas can create the channel state information with large dimension for each location. By utilizing a matched filter based precoder or equalizer, the signal energy can concentrate on the corresponding location [8]. On the other hand, the wide bandwidth can help reveal multiple paths in a rich scattering environment, e.g., the scenarios of indoor or dense metropolis. By utilizing the time reversal (TR) technology [9], the signal energy can also concentrate on the intended location, generating the spatial focusing effect.

This common spatial focusing phenomenon creates a tunnelling effect for each user at his/her own location, such that the interference among different users are rather weak. Thus, multiple users can concurrently conduct data transmission upon the entire spectrum by utilizing their corresponding channel state information as a unique signature. In essence, their locations have ideally separated them in the spatial domain and each different location is just a spatial "white space". Therefore, this emerging spatial focusing effect enables us to develop a general spatial spectrum sharing scheme, which allows the reuse of the entire spectrum, instead of separating users either in time domain or in the spectrum domain like the traditional dynamic spectrum access technology.

The remaining of this paper is organized as follows. Section II presents the system models for both TR wideband and massive MIMO systems. Then, we analyze the SINR performance for both systems in Section III. Simulation results are shown in Section IV and conclusions are drawn in Section V.

2. SYSTEM MODELS

2.1. Time Reversal Wideband System

In the TR wideband system, suppose there are M base stations (BSs) each equipped with Φ_t antennas, and N user equipment (UEs) each with a single antenna. The channel between the ϕ_t-th antenna of the i-th BS and the j-th UE can be modeled by the large scale fading incurred by the distance attenuation combined the small scale fading incurred by the multi-path environment. The small scale fading, denoted by $\mathbf{h}_{i,j}^{\phi_t}$, can be written by

$$\mathbf{h}_{i,j}^{\phi_t} = \left[h_{i,j}^{\phi_t}[0], h_{i,j}^{\phi_t}[1], \ldots, h_{i,j}^{\phi_t}[L-1] \right], \tag{1}$$

where $h_{i,j}^{\phi_t}[k]$ represents the k-th tap of the channel impulse response (CIR) with length L and can be written by

$$h_{i,j}^{\phi_t}[k] = \sum_{l=0}^{L-1} h_{i,j}^{\phi_t,l} \delta[k-l], \tag{2}$$

with $\delta[\cdot]$ as the Dirac delta function.

For the j-th UE, let us denote A_j as the BS that the UE is associating with and denote $\mathcal{N}_{A_j}$ as the current set of UEs that are associating with BS A_j besides the j-th UE. The intended message for those UEs belonging to $\mathcal{N}_{A_j}$ can be represented by $\{X_j, X_{j' \in \mathcal{N}_{A_j}}\}$, where each of the sequence of information symbols X_j or $X_{j'}$ are independent complex random variables with zero mean and $\mathbb{E}\left[|X_{j,j'}[k]|^2 \right] = 1$. This sequence of message is first up-sampled by the back-off factor D into $\{X_j^{[D]}, X_{j' \in \mathcal{N}_{A_j}}^{[D]}\}$ for the sake of alleviating the inter-symbol interference due to the delay spread. The up-sampled sequence is then convoluted with the signature generated by the CIRs. After that, all the convoluted messages are added up and transmitted into wireless channels. The transmission power of each BS's antenna is regarded as identical P, and the power allocation for the j-th TD can be denoted by $P_{A_j,j}$, where it should be satisfied that $P_{A_j,j} + \sum_{j' \in \mathcal{N}_{A_j}} P_{A_j,j'} = P$. In such a case, the transmission signal on the ϕ_t-th antenna of BS A_j can be written by

$$S_{A_j}^{\phi_t}[k] = \sqrt{P_{A_j,j}} \left(X_j^{[D]} * g_{A_j,j}^{\phi_t} \right)[k] + \sum_{j' \in \mathcal{N}_{A_j}} \sqrt{P_{A_j,j'}} \left(X_{j'}^{[D]} * g_{A_j,j'}^{\phi_t} \right)[k] \tag{3}$$

where $g^\phi_{A_j,j}$ is the signature between the ϕ-th antenna of BS A_j and the j-th UE. If considering basic TR signature, $g^\phi_{A_j,j}$ should be:

$$g_{A_j,j}[k] = \frac{h^*_{A_j,j}[L-1-k]}{\sqrt{\mathbb{E}\left[\sum_{l=0}^{L-1}\left|h_{A_j,j}[l]\right|^2\right]}}, \tag{4}$$

which is the normalized (by the average channel gain) complex conjugate of time reversed $\{h^*_{A_j,j}[k]\}$.

For the receiver side of the TR wideband system, the received signal of the j-th UE can be represented as follows

$$Y^{[D]}_j[k] = \sum_{i=1}^{M}\sum_{\phi_t=1}^{\Phi_t} d_{i,j}^{-\alpha/2}\left(S_i^{\phi_t} * h_{i,j}^{\phi_t}\right)[k] + n_j[k], \tag{5}$$

where $d_{i,j}$ represents the distance, α is the path loss coefficient, and n_j represents the additive white Gaussian noise with variance σ^2.

2.2. Massive MIMO System

In the massive MIMO system, suppose there are M BSs each associated with a massive number of antennas Φ_m, and N UEs each with a single antenna with $1 \ll N \ll \Phi_m$. For the simplicity of expression, we assume flat fading for each antenna [10]:

$$\mathbf{H}_i = \{\mathbf{h}^T_{i,1}, \mathbf{h}^T_{i,2}, \ldots, \mathbf{h}^T_{i,|\mathcal{N}_i|}\}, \tag{6}$$

where $\mathcal{N}_i$ represents the set of UEs that associate with the i-th BS and the number of UEs in $\mathcal{N}_i$ is denoted as $|\mathcal{N}_i|$. In such a case, we have $\mathbf{H}_i \in \mathbb{C}^{\Phi_m \times |\mathcal{N}_i|}$, i.e., $\mathbf{h}_{i,j} \in \mathbb{C}^{1 \times \Phi_m}$ is the small-scale fading channel between the i-th BS and the j-th UE in $\mathcal{N}_i$. Here, the CSI is assumed to be perfectly known by the BSs. Let us denote the beamforming matrix of the i-th BS as $\mathbf{G}_i = \{\mathbf{g}_{i,1}, \mathbf{g}_{i,2}, \ldots, \mathbf{g}_{i,|\mathcal{N}_i|}\}$, where $\mathbf{G}_i \in \mathbb{C}^{\Phi_m \times |\mathcal{N}_i|}$ and $\mathbf{g}_{i,j} \in \mathbb{C}^{\Phi_m \times 1}$. Suppose $\mathbf{s}_i = [s_{i,1}, s_{i,2}, \ldots, s_{i,|\mathcal{N}_i|}]^T$ is the transmit symbols of the i-th BS with length determined by the number of UEs that associate with it, where $\mathbf{s}_i \in \mathbb{C}^{|\mathcal{N}_i| \times 1}$ and $\mathbb{E}(\mathbf{s}_i\mathbf{s}_i^*) = \mathbf{I}$. Thus, the received signal of the j-th TD can be expressed by

$$Y_j = \sum_{i=1}^{M} \sqrt{P} d_{i,j}^{-\alpha/2} \mathbf{h}_{i,j}\mathbf{G}_i\mathbf{s}_i + n_j, \tag{7}$$

where P represents the transmission power of each antenna, $d_{i,j}$ represents the distance between the i-th BS and the j-th UE, α is the path loss coefficient, $d_{i,j}^{-\alpha/2}$ represents the large scale attenuation, and n_j represents the additive white Gaussian noise with zero mean and variance σ^2.

3. SPATIAL FOCUSING EFFECT

3.1. Ray-Tracing based Simulation

As aforementioned, both TR wideband and massive MIMO systems can exhibit this spatial focusing effect. However, the approaches are different where the TR system relies on a wide bandwidth but the massive MIMO system relies on a large number of antennas. For the TR wideband system in a rich scattering environment with multi-path propagation (e.g., dense city or indoor scenarios), the wide bandwidth can help reveal those multiple paths from the transmitter to each specific location. The wider bandwidth can reveal more multi-paths for each location, and thus can lead to less correlation between every two different locations' channels. Eventually, by utilizing the time-reversed CIR of a specific location as the waveform of this location, the convolution of the waveform and
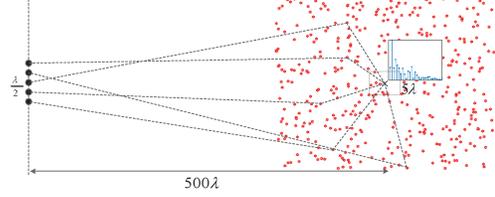

Fig. 1. Simulation setup for validating spatial focusing effect.

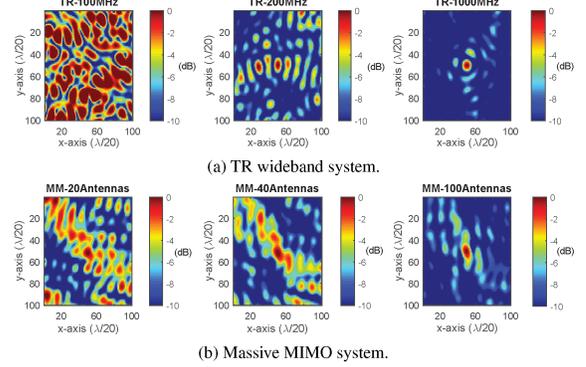(a) TR wideband system.

(b) Massive MIMO system.

Fig. 2. Spatial focusing effect of both systems.

the channel can generate a unique peak at that specific location, with little energy leakage to the neighboring locations. For the massive MIMO system equipped with a large scale of antennas, those antennas can physically create a large dimension of CSI for each location, which also leads to the small correlation among difference locations. Therefore, by utilizing a simple matched filter precoder based on the CSI of a specific location, the signal energy can be spatially focused at that specific location.

To validate this spatial focusing effect, we construct a ray-tracing based simulation in a discrete scattering environment. As shown in Fig. 1, a total number of 400 effective scatters are distributed randomly in a square area with dimension $200\lambda \times 200\lambda$, where λ is the wavelength corresponding to the carrier frequency. In such a case, the wireless channel can be represented as a sum of multi-paths using the classical ray-tracing method. Without loss of generality, we adopt a single-bounce ray-tracing model in computing the channel impulse responses in both TR wideband and the large scale antenna array systems, where both systems are operated on 5GHz ISM band. The reflection coefficient of each scatter is chosen to be I.I.D. complex random variables with uniform distribution both in amplitude (from 0 to 1) and phase (from 0 to 2π). For the large antenna array system as show in Fig. 1, the antennas are placed in a line facing the scattering area and the interval between each two antennas is $\lambda/2$. Moreover, the distance between the transmitter and the intended location is chosen to be 500λ.

In the simulation, for the TR wideband system, it is assumed to be equipped with only a single antenna, and the bandwidth is tuned from 100 MHz to 500 MHz. By contrast, for the large antenna array system, the number of antennas is adjusted from 20 to 100, while the bandwidth of the system is fixed to be 1 MHz. This narrow-band configuration guarantees that the CIR has a single tap, which is a common assumption in OFDM-based massive MIMO literature [8]. In order to achieve the energy concentration at the intended location,
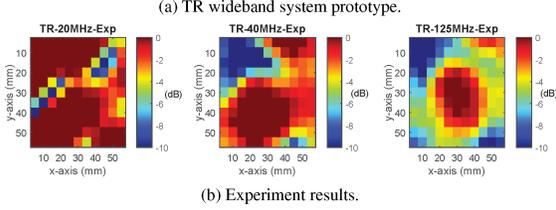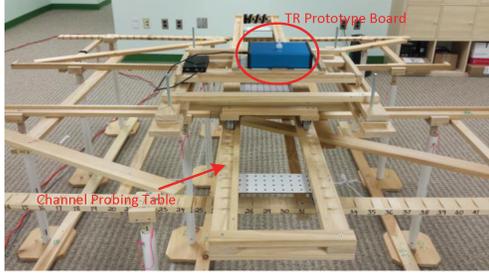
(a) TR wideband system prototype.

(b) Experiment results.

Fig. 3. Spatial focusing effect of TR wideband system prototype.

time-reversal mirror precoder and matched filter based precoder are applied in TR wideband and large antenna array systems, respectively. As shown in Fig. 1, we consider the field strengths around the intended location with dimension $5\lambda \times 5\lambda$. Fig. 2 shows the simulation results of both systems, where the maximal received signal strength is set to be 0dB for normalization. We can clearly see that for the TR wideband system, the spatial focusing effect can be improved with wider and wider bandwidth. Similarly, for the large antenna array system, the increasing number of antennas can also lead to better spatial focusing effect.

3.2. Prototype based Experiment

To further verify the spatial focusing effect, we built a prototype of TR wideband system on a customized software-defined radio (SDR) platform, as shown in Fig. 3-(a). The hardware architecture combines a specific designed radio-frequency board covering the ISM band with 125 MHz bandwidth, a high-speed Ethernet port, and an off-the-shelf user-programmable module board. In this experiment, we measure the CIRs of a square region with dimension 5cm × 5cm on a channel probing table which is located in a typical office environment as shown in Fig. 3. The intended location is chosen to be the center of the measured region and the corresponding normalized field strength is shown in Fig. 3-(b). We can see that the TR transmission can generate a clear energy focusing around the intended location, even under a not-so-wide bandwidth of 125 MHz. Relying on this spatial focusing effect, the UEs at different locations can be ideally separated, which enables the concurrent data transmission over the entire spectrum.

4. SPATIAL SPECTRUM SHARING PERFORMANCE

Although the spatial focusing effect can help separate multi-users' simultaneous transmission, the non-ideal uncorrelated channels can still lead to minor inference to each other. Hence, we quantify such interference for both systems in this section as well as the effective SINR performance. As we will see later, an interesting phenomenon shows that the SINR expression of both TR wideband and massive MIMO systems share the same formulation, which is fundamentally

due to the similar spatial focusing effect existing in both systems.

4.1. Time Reversal Wideband System

Let us consider the multi-user downlink transmission of a TR wideband system. The j-th UE just simply performs a one-tap gain adjustment a_j to the received signal to recover the signal and then down-samples it with the same back-off factor D. Thus, the received signal of the j-th UE, denoted by $Y_j[k]$, can be written as follows:

$$Y_j[k] = a_j \sum_{i=1}^{M} \sum_{l=0}^{(2L-2)/D} \sum_{\phi_t=1}^{\Phi_t} d_{i,j}^{-\alpha/2} \Big(S_i^{\phi_t} * h_{i,j}^{\phi_t} \Big)[Dl] + a_j n_j[k]. \tag{8}$$

To better understand $Y_j[k]$, we further re-write it:

$$Y_j[k] = a_j \sum_{\phi=1}^{\Phi_t} \sqrt{P_{A_j,j}} X_j[k] \cdot d_{A_j,j}^{-\alpha/2} \left(h_{A_j,j}^{\phi} * g_{A_j,j}^{\phi} \right)[L-1] +$$

$$a_j \sum_{\substack{l=0 \\ l \neq (L-1)/D}}^{(2L-2)/D} \sum_{\phi=1}^{\Phi_t} \sqrt{P_{A_j,j}} X_j[k-l] \cdot d_{A_j,j}^{-\alpha/2} \left(h_{A_j,j}^{\phi} * g_{A_j,j}^{\phi} \right)[Dl] +$$

$$a_j \sum_{j' \in \mathcal{N}_{A_j}} \sum_{l=0}^{(2L-2)/D} \sum_{\phi=1}^{\Phi_t} \sqrt{P_{A_j,j'}} X_{j'}[k-l] d_{A_j,j}^{-\alpha/2} \Big(h_{A_j,j}^{\phi} * g_{A_j,j'}^{\phi} \Big)[Dl] +$$

$$a_j \sum_{j' \notin \mathcal{N}_{A_j}} \sum_{l=0}^{(2L-2)/D} \sum_{\phi=1}^{\Phi_t} \sqrt{P_{A_{j'},j'}} X_{j'}[k-l] d_{A_{j'},j}^{-\alpha/2} \left(h_{A_{j'},j}^{\phi} * g_{A_{j'},j'}^{\phi} \right)[Dl]$$

$$+ a_j n_j[k], \tag{9}$$

where the first term is the intended signal, the second term is the inter-symbol interference (ISI), the third term is the inter-user interference (IUI) caused by the UEs that share the same BS, and the fourth term is the inter-cell interference (ICI).

Theorem 1: The SINR performance of the TR wideband system, when the equal power allocation and the time reversal waveform are applied, is as follows

$$\text{SINR}_j = \frac{\xi_1}{\xi_2 + \xi_3 \left(\left| \mathcal{N}_{A_j} \right| + 1 \right) d_{A_j,j}^{\alpha}}, \tag{10}$$

$$\xi_1 = \frac{1 + e^{-\frac{LT_s}{\sigma_T}}}{1 + e^{-\frac{T_s}{\sigma_T}}} + \frac{1 - e^{-\frac{LT_s}{\sigma_T}}}{1 - e^{-\frac{T_s}{\sigma_T}}}, \tag{11}$$
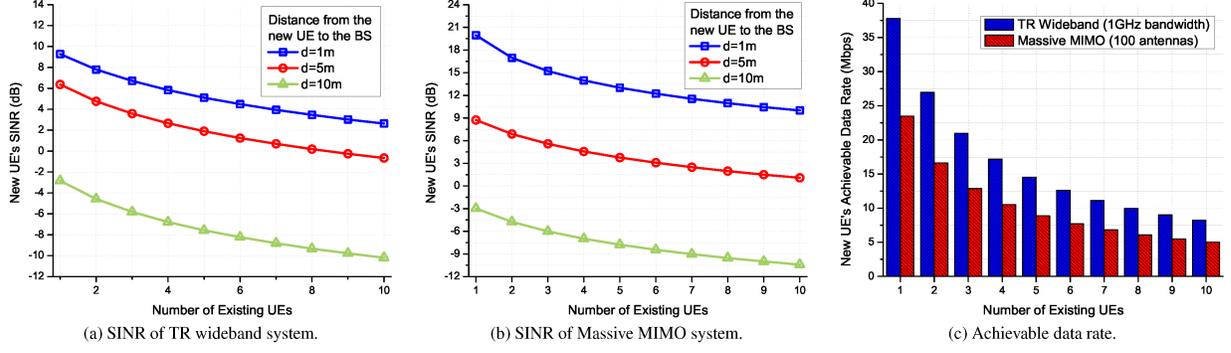
$$\xi_2 = 2 \frac{e^{-\frac{T_s}{\sigma_T}} \left(1 - e^{-\frac{(L-2+D)T_s}{\sigma_T}} \right)}{\left(1 - e^{-\frac{DT_s}{\sigma_T}} \right) \left(1 + e^{-\frac{T_s}{\sigma_T}} \right)} - \tag{12}$$

$$\frac{\left(1 + e^{-\frac{DT_s}{\sigma_T}} \right) \left(1 + e^{-\frac{2LT_s}{\sigma_T}} \right) - 2 e^{-\frac{(L+1)T_s}{\sigma_T}} \left(1 + e^{-\frac{(D-2)T_s}{\sigma_T}} \right)}{\left(1 - e^{-\frac{DT_s}{\sigma_T}} \right) \left(1 + e^{-\frac{T_s}{\sigma_T}} \right) \left(1 - e^{-\frac{LT_s}{\sigma_T}} \right)},$$

$$\xi_3 = \sigma_j^2/P + \sum_{i=1}^{M} d_{i,j}^{-\alpha} \cdot \tag{13}$$

$$\frac{\left(1 + e^{-\frac{DT_s}{\sigma_T}} \right) \left(1 + e^{-\frac{2LT_s}{\sigma_T}} \right) - 2 e^{-\frac{(L+1)T_s}{\sigma_T}} \left(1 + e^{-\frac{(D-2)T_s}{\sigma_T}} \right)}{\left(1 - e^{-\frac{DT_s}{\sigma_T}} \right) \left(1 + e^{-\frac{T_s}{\sigma_T}} \right) \left(1 - e^{-\frac{LT_s}{\sigma_T}} \right)}.$$

Proof: Due to the page limit, please find the prove in the supplementary file [11].

(a) SINR of TR wideband system. (b) SINR of Massive MIMO system. (c) Achievable data rate.

Fig. 4. SINR and rate performance of both systems. Simulation settings: 3 BSs, SNR=20dB, path loss $\alpha = 4$.

4.2. Massive MIMO System

Let us consider the multi-user downlink transmission of a massive MIMO system. Since the BSs have performed beamforming based on the CSI, the UE can simply do the one-tap detection to receive the signal. Similar to the TR wideband system, the received signal of the j-th UE can be formulated by the summation of the intended signal, IUI and ICI, as follows:

$$
\begin{aligned}
y_j &= \sum_{i=1}^{M} \sqrt{P} d_{i,j}^{-\alpha/2} \mathbf{h}_{i,j} \mathbf{G}_i \mathbf{s}_i + n_j \\
&= \sqrt{P_{A_j,j}} d_{A_j,j}^{-\alpha/2} \mathbf{h}_{A_j,j} \mathbf{g}_{A_j,j} s_{A_j,j} + \\
&\quad \sum_{j' \in \mathcal{N}_{A_j}} \sqrt{P_{A_j,j'}} d_{A_j,j}^{-\alpha/2} \mathbf{h}_{A_j,j} \mathbf{g}_{A_j,j'} s_{A_j,j'} + \\
&\quad \sum_{\substack{i=1 \\ i \neq A_j}}^{M} \sqrt{P} d_{i,j}^{-\alpha/2} \mathbf{h}_{i,j} \mathbf{G}_i \mathbf{s}_i + n_j,
\end{aligned}
\tag{14}
$$

where A_j denotes the BS that the j-th TD will associate with, $\mathbf{h}_{A_j,j}$ denotes the CSI between the BS and the j-th UE, $s_{A_j,j}$ denotes the intended symbol for the j-th UE, $\mathbf{g}_{A_j,j}$ denotes the beamforming vector for the j-th UE, $\mathcal{N}_{A_j}$ denotes the current set of TDs that also associate BS A_j besides the j-th UE, and n_j represents the noise. In the last equality of (14), the first term is the intended signal for the j-th UE, while the second term is the IUI and the third term is the ICI for the j-th UE.

Theorem 2: The SINR performance of the massive MIMO system, when the equal power allocation and the maximum ratio combining (MRC) beamforming are applied, is as follows:

$$
\text{SINR}_j = \frac{\xi_1'}{\xi_2' + \xi_3' \left(\left| \mathcal{N}_{A_j} \right| + 1 \right) d_{A_j,j}^{\alpha}},
\tag{15}
$$

$$
\xi_1' = (\Phi_m + 1)\gamma, \quad \xi_2' = -\gamma, \quad \xi_3' = \sum_{i=1}^{M} d_{i,j}^{-\alpha}\gamma + \sigma_j^2/P.
\tag{16}
$$

Proof: Due to the page limit, please find the prove in the supplementary file [11].

5. SIMULATION RESULTS

In this section, we conduct simulation to evaluate the performance of the spatial spectrum sharing. The systems are set as 1 GHz for the TR wideband system with a single antenna, and as 40 MHz for the massive MIMO system with 100 transmission antennas. For the TR wideband system, the sampling period $T_s = 1$ ns, back off factor $D = 16$, the channel length is typically $L = 256$ and the root mean square delay spread is typically $\sigma_T = 128 T_s$, according to the IEEE 802.15.4a outdoor non-line-of-sight channels. While for the massive MIMO system, OFDM technology is adopted for each antenna and each subcarrier is considered to be with channel length $L = 1$.

Fig. 4-(a,b) shows the SINR performance of the new arrival UE in both TR wideband and massive MIMO systems under different numbers of existing UEs in the associated BS, i.e., from 1 UE to 10 UEs. The distance between the new UE and the associated BS is configured as 1m, 5m and 10m, respectively, which are corresponding to the three curves in each sub-figure of Fig. 4. The distances between the new UE and the other two interference BSs are set as 20m. Generally, the results in both sub-figures show that when the number of existing UEs increases, i.e., the associated BS becomes more and more crowded, the SINR of each individual UE decreases due to the power sharing and IUI. Meanwhile, the farther distance between the new UE and the associated BS can also lead to decreased SINR due to the path loss. Moreover, we also show the numerical achievable data rate of the new UE in Fig. 4-(c). Note that the TR wideband data rate is calculated by $B/D \log(1 + \text{SINR})$ and the massive MIMO data rate is calculated by $B \log(1 + \text{SINR})$. It can be seen that both systems can achieve equivalently high throughput either by wide bandwidth for TR wideband or by a large number of antennas for massive MIMO.

6. CONCLUSIONS

In this paper, we proposed a general spatial spectrum sharing architecture based on the spatial focusing characteristic in both TR wideband and massive MIMO systems. Relying on this spatial focusing phenomenon phenomenon, we analyzed the SINR performance of concurrently spatial spectrum sharing for both TR wideband and massive MIMO systems. It turned out to be that the SINR of both systems shared exactly the same expression under the equal power allocation scenario. To summarize, with the trends of wider bandwidth and larger scale of antennas, spatial focusing effect becomes the uniqueness of next generation networks. This effect can be a bridge that separates the physical layer and MAC layer design, where the physical layer design should focus on how to strengthen this focusing effect in order to alleviate interference, while the MAC layer design should concentrate on how to utilize this effect to accommodate more users.

7. REFERENCES

[1] B. Wang and K. J. R. Liu, "Advances in cognitive radio networks: A survey," *IEEE J. Sel. Topics Signal Process.*, vol. 5, no. 1, pp. 5–23, Feb. 2011.

[2] G. Ding, J. Wang, Q. Wu, Y.-D. Yao, R. Li, H. Zhang, and Y. Zou, "On the limits of predictability in real-world radio spectrum state dynamics: from entropy theory to 5g spectrum sharing," *IEEE Commun. Mag.*, vol. 54, no. 7, pp. 178–183, Jul. 2015.

[3] A. M. Akhtar, X. Wang, and L. Hanzo, "Synergistic spectrum sharing in 5g hetnets: A harmonized sdn-enabled approach," *IEEE Commun. Mag.*, vol. 54, no. 1, pp. 40–47, Jan. 2016.

[4] B. Li, S. Li, A. Nallanathan, and C. Zhao, "Deep sensing for future spectrum and location awareness 5g communications," *IEEE J. Sel. Areas Commun.*, vol. 33, no. 7, pp. 1331–1344, Jul. 2015.

[5] J. M. III, J. Guerci, J. Reed, Y.-D. Yao, Y. Chen, T. C. Clancy, ohanna Dwyer, H. Li, H. Man, R. McGwier, and Y. Guo, "Accelerating 5g qoe via public-private spectrum sharing," *IEEE Commun. Mag.*, vol. 52, no. 5, pp. 77–85, May. 2014.

[6] D. W. K. Ng, M. Breiling, C. Rohde, F. Burkhardt, and R. Schober, "Energy-efficient 5g outdoor-to-indoor communication: Sudas over licensed and unlicensed spectrum," *to appear in IEEE Trans. Wirelss Commun.*, 2016.

[7] B. Singh, S. Hailu, K. Koufos, A. A. Dowhuszko, O. Tirkkonen, R. Jntti, and R. Berry, "Coordination protocol for interoperator spectrum sharing in co-primary 5g small cell networks," *IEEE Commun. Mag.*, vol. 53, no. 7, pp. 34–40, Jul. 2015.

[8] F. Rusek, D. Persson, B. K. Lau, E. G. Larsson, T. L. Marzetta, O. Edfors, and F. Tufvesson, "Scaling up mimo: Opportunities and challenges with very large arrays," *IEEE Signal Process. Mag.*, vol. 30, no. 1, pp. 40–60, Jan. 2013.

[9] B. Wang, Y. Wu, F. Han, Y. H. Yang, and K. J. R. Liu, "Green wireless communications: A time-reversal paradigm," *IEEE J. Sel. Areas Commun.*, vol. 29, no. 8, pp. 1698–1710, Sep. 2011.

[10] H. Q. Ngo, E. G. Larsson, and T. L. Marzetta, "Energy and spectral efficiency of very large multiuser mimo systems," *IEEE Trans. Commun.*, vol. 61, no. 4, pp. 1436–1449, Apr. 2013.

[11] C. Jiang, B. Wang, Y. Han, Z. Wu, and K. J. R. Liu, "Supplementary information," [Online]. Available: http://www.jiangchunxiao.net/spicassp17.pdf.